

An Autonomous Water-Dropping Method with High Precision using Unmanned Aerial Firefighting Vehicles

Xiaobo Wu¹, Shun Li¹, Linhan Qiao¹ Youmin Zhang¹, Hamza Benzerrouk² and Hakim Guiddir²

Abstract—The water-dropping method is crucial for the aerial firefighting using either fixed-wing or rotary-wing aircraft. When a wildfire occurs, aerial firefighters need to cross the wildfire and extinguish it by dropping water/retardant based on their experiences. It is extremely dangerous for aerial firefighters to carry out such a mission with also the lack of water-dropping accuracy while mainly based on pilot's experience. In order to improve the precision of water-dropping and reduce the risk to firefighters in aerial firefighting missions, an autonomous water-dropping method with high precision has been proposed for fire spot suppression using unmanned rotary-wing aerial firefighting vehicles. Once a fire spot location is determined, the unmanned aerial firefighting vehicle will fly to and hover above the fire spot based on GPS navigation information autonomously. Then a feedback controller drives the unmanned aerial firefighting vehicle to approach the fire spot quickly based on the relative distance difference perceived by an infrared thermal camera. Meanwhile, a wireless trigger is utilized to execute the drop action when the precision or time conditions for water-dropping are met. Finally, the unmanned aerial firefighting vehicle returns to the ground station safely. The designed method implemented and tested in the outdoor field with a DJI M300 quadrotor unmanned aerial vehicle equipped with an onboard H20T payload. The experiment results have demonstrated the effectiveness of the designed method.

Index Terms—Wildfires, unmanned aerial firefighting vehicles, infrared thermal camera, feedback controller.

I. INTRODUCTION

Wildfire can burn combustible vegetation in an area. It greatly impacts the natural environment including water security, the atmosphere and ecosystems [1]–[3]. At the same time, it also has affected human health directly or indirectly [4]. Fig. 1 shows a diagram of classical aerial firefighting scenarios. When a wildfire occurs, in addition to ground firefighting which is limited, aerial firefighting is an important and efficient resource to combat wildfires. The modified aircraft used for aerial firefighting includes fixed-wing aircraft with a tank and helicopters with a Bambi bucket generally. They are the fastest and most effective means of initial wildfire attack. They are also excellent at covering large areas. Besides, aircraft can be used to monitor fires and provide real-time fireground status for firefighting crews.

¹Xiaobo Wu, Shun Li, Linhan Qiao and Youmin Zhang (Corresponding Author) are with the Department of Mechanical, Industrial and Aerospace Engineering, Concordia University, Montreal, Quebec H3G 1M8, Canada (wu_xiaob@live.concordia.ca, li_shun@live.concordia.ca, q_linhan@live.concordia.ca, youmin.zhang@concordia.ca)

²Hamza Benzerrouk and Hakim Guiddir are with the Rotors&Wings Aerogroup, Saint-Hubert, Quebec, J3Y 8Y9, Canada (h.benzerrouk@rwaerogroup.com, h.guiddir@rwaerogroup.com)



Fig. 1. The diagram about how to attack wildfires in aerial firefighting.

Perception and recognition are the first steps in aerial firefighting. Many effective methods have been developed. Review paper [5] summarized a comparison of four methods that have been used for forest fire detection with exhaustive surveys of their techniques. They include human-based observation, satellite systems, optical cameras and wireless sensor networks. Paper [6] proposed a system and methodology that can be used to detect forest fires at the initial stage using a wireless sensor network. Paper [7] proposed a novel method of detecting forest fire using color and multi-color space local binary pattern of both flame and smoke signatures and a single artificial neural network. How to efficiently and accurately drop water above the fire spots is also a key problem for aerial firefighting. Paper [8] proposed a fast optimization method of a water-dropping scheme for fixed-wing firefighting aircraft. The application of examples also shows that the method can optimize the water-dropping scheme quickly instead of aircrew experience and play the role of auxiliary decision support for the firefighting mission of fixed-wing firefighting aircraft. Paper [9] examines the potential use of fire extinguishing balls as part of the proposed system, where drone and remote-sensing technologies are utilized cooperatively. The results of the experiments guided the authors towards wildfire fighting rather than building fires. Paper [10] presents a systematic overview of UAV-based forest fire fighting technology progress including UAV forest fire monitoring, detection, fighting and existing

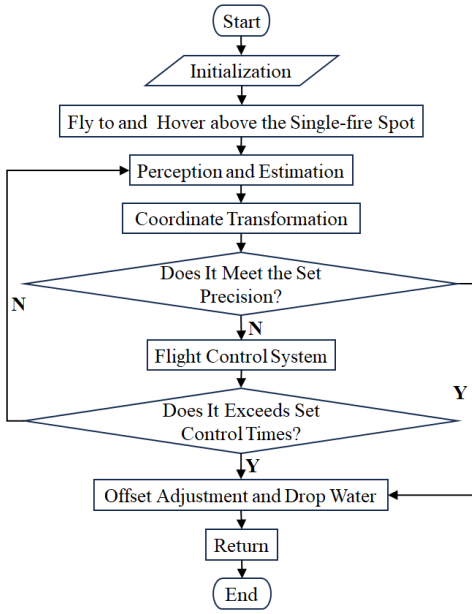


Fig. 2. The whole process of high-precision water-dropping method with high-precision.

challenges.

However, previous research has only focused on wildfire detection or the water-dropping scheme for aircraft with aerial firefighters for fixed-wing firefighting aircraft. Few works have addressed the problem of how to drop water with high accuracy using unmanned aerial firefighting vehicles (UAFVs). In this paper, a high-precision water-dropping method using UAFVs based on a feedback controller has been proposed. The methodology is illustrated in Section II. The corresponding aerial firefighting system is designed and the aerial firefighting testing result is analyzed in Section III. Finally, Section IV summarizes the paper and prospects the future work.

II. METHODOLOGY

The whole process of the autonomous water-dropping method with high precision using a UAFV is outlined in Fig. 2. First, the UAFV will fly to and hover above the single fire spot based on GPS navigation from the ground station when receiving a fire suppression task. This process ensures that the fire spot can appear in the field of the infrared thermal (IR) camera and be captured by the IR camera. Second, a feedback controller with the IR camera is designed based on the real-time horizontal position error between the center of the fire spot and the center of the IR camera. The UAFV is actuated to approach quickly to the fire spot in the horizontal direction. When the horizontal position error meets the pre-set requirement, the program will proceed to the next stage. This process ensures that the center of the IR camera is right above the center of the fire point. Or when the time exceeds the pre-set time, the UAFV will return to the ground station directly. Third, when the real precision meets the pre-set precision requirement, the dropping water action is triggered after the known offset between the IR

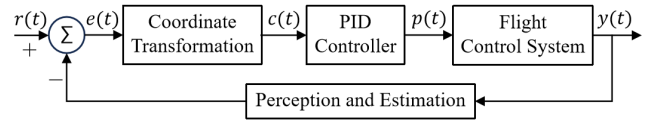


Fig. 3. The feedback controller based on infrared thermal camera.

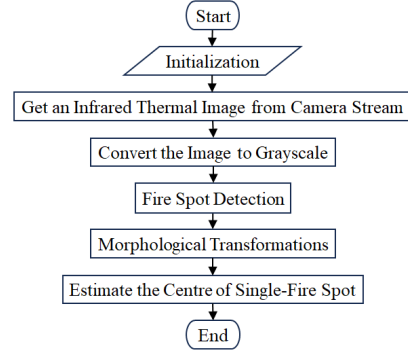


Fig. 4. The procedure of detecting fire and estimating the center point of the fire spot.

camera and the tank outlet is released for water dropping. The offset adjustment ensures that the center of the fire point is located right below the water tank outlet. Finally, the UAFV returns to the ground station autonomously. Since the feedback controller is the key to the whole process of the high-precision water-dropping method, it will be introduced and described in detail below. The diagram of the feedback controller of the high-precision water-dropping method is shown in Fig. 3 which consists of four parts: the perception and estimation, the PID controller, the coordinate transformation and the flight control system.

A. Perception and Estimation

The perception and estimation refer to computer vision technologies that are utilized to detect the fire spot and estimate the center position of the fire spot based on the IR camera. Such a procedure is showed in Fig. 4.

First, the IR camera is set to face the ground vertically by controlling the gimbal and grab a real-time infrared thermal image (IR image). Since the IR image can only record different levels of infrared light [11] and the value of each pixel represents the intensity information of light in the grayscale image [12], the IR image can be converted to the grayscale image with a different value of pixel and the fire spot can be detected with the feature of a higher level of light. Given the fact that the grayscale image from IR image has only two distinct values where the fire spot has a higher intensity of light than the environment around it, then the Otsu's method [13] that determines an optimal global threshold value is utilized to detect the fire spot in the environment. After that, morphological transformations are usually needed including erosion and dilation [14]. Erosion can remove white noises, but it also shrinks the fire spot. In order to overcome the problem, erosion is followed by dilation. Since the noise is gone, it would not come back

anymore, when the fire spot area increases. At last, the center position of the fire spot area in pixel coordinate needs to be estimated. A feasible method is to use a bounding box to catch the fire spot area with an adaptive size and regard the center position of the bounding box as the estimated center of the fire spot. In order to do this, the contours of the fire spot must be identified [15] and a rectangle is created [16] around the fire spot.

B. Coordinate Transformation

The reason why the pixel error $e(t)$ between the estimated center point of the fire spot and the principal point of the IR camera in the pixel coordinate is converted to the horizontal position error $c(t)$ in the camera coordinate is that the PID controller needs to use the $c(t)$ as the input parameter to control the UAFV as demonstrated in Fig. 3.

Fig. 5 shows the diagram of the coordinate transformation. There are four type of coordinate systems, including pixel coordinate $O_p - uv$, image coordinate $O_i - xy$, camera coordinate $O_c - X_c Y_c Z_c$ and world coordinate $O_w - X_w Y_w Z_w$ which are all consistent with the right-hand rule. The world coordinate system used for the UAFV aligns the positive X_w , Y_w and Z_w axes with the directions of North, East and Down. This convention is called North-East-Down. The UAFV hovers above the fire spot area and keeps a fixed altitude and attitude of facing the north in the world coordinate system. Meanwhile, the IR camera keeps facing the fire ground vertically. It means that the principal axis is facing the fire ground vertically. The square region $ABCD$ is perceived by the IR camera. The G point is the real-time center of the fire spot and the E point is the projection point of the IR camera focal point O_c . The O_i is the origin and F is the estimated center of the fire spot in the image coordinate system. Because when the E and G points coincide, the IR camera is located right over the center of fire spot, the error e_{GE} between E point and G point can be regarded as input error of the feedback controller. Based on the error e_{FO_i} between F and the origin O_i , the error e_{EG} will be obtained by coordinate transformation. Camera calibration is a necessary step in 3D computer vision to extract metric information from 2D images [17]. The IR camera would be calibrated before coordinate transformation [18]–[21]. Then the coordinate transformation from pixel coordinate to image coordinate is following: Firstly, suppose the F point is (x, y) in the image coordinate system. $O_i(x_0, y_0)$ is the principal point in the pixel coordinate system, the relationship between image coordinate and pixel coordinate can be viewed in (1):

$$\begin{aligned} u &= \frac{x}{dx} + x_0 \\ v &= \frac{y}{dy} + y_0 \end{aligned} \quad (1)$$

where d_x, d_y are length and width of the single pixel, (u, v) is the corresponding point in the pixel coordinate of the point F , and the corresponding matrix is as following (2):

$$\begin{bmatrix} u \\ v \\ 1 \end{bmatrix} = \begin{bmatrix} 1/dx & 0 & x_0 \\ 0 & 1/dy & y_0 \\ 0 & 0 & 1 \end{bmatrix} \begin{bmatrix} x \\ y \\ 1 \end{bmatrix} \quad (2)$$

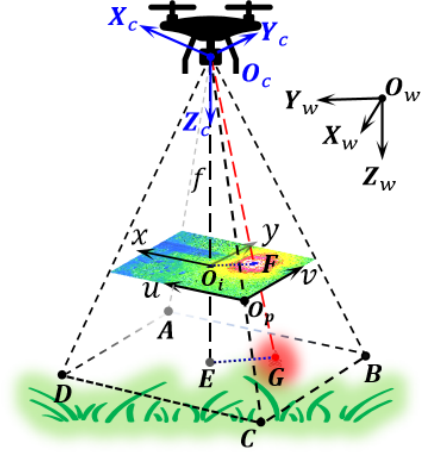


Fig. 5. The diagram of the coordinate transformation.

Secondly, the $F(x, y)$ in the image coordinate will be converted to $G(x_c, y_c, z_c)$ in the camera coordinate. According to the similar triangles principal, following equation can be obtained (3):

$$\frac{x_c}{x} = \frac{y_c}{y} = \frac{z_c}{f} \quad (3)$$

where the f is focal length, z_c is called the depth that is the distance between point O_c and E and $O_c Z_c$ is the optic axis, and the corresponding matrix of (3) is (4):

$$z_c \begin{bmatrix} x \\ y \\ 1 \end{bmatrix} = \begin{bmatrix} f & 0 & 0 \\ 0 & f & 0 \\ 0 & 0 & 1 \end{bmatrix} \begin{bmatrix} x_c \\ y_c \\ z_c \end{bmatrix} \quad (4)$$

So, the G point is (x_c, y_c, z_c) meeting equation (5):

$$\begin{bmatrix} x_c \\ y_c \\ z_c \end{bmatrix} = z_c \begin{bmatrix} 1/f & 0 & 0 \\ 0 & 1/f & 0 \\ 0 & 0 & 1 \end{bmatrix} \begin{bmatrix} dx & 0 & -x_0 dx \\ 0 & dy & -y_0 dy \\ 0 & 0 & 1 \end{bmatrix} \begin{bmatrix} u \\ v \\ 1 \end{bmatrix} \quad (5)$$

It is obvious that the error between the point E and the point G in the camera coordinate meets equation (6):

$$\begin{bmatrix} \Delta x \\ \Delta y \end{bmatrix} = z_c \begin{bmatrix} 1/f & 0 \\ 0 & 1/f \end{bmatrix} \begin{bmatrix} dx & 0 & -x_0 dx \\ 0 & dy & -y_0 dy \end{bmatrix} \begin{bmatrix} \Delta u \\ \Delta v \\ 1 \end{bmatrix} \quad (6)$$

The error Δx and Δy are the $c(t)$. The pixel error Δu and Δv corresponds to $e(t)$ in Fig. 3.

C. PID Controller

Proportional-Integral-Derivative (PID) control is the most commonly used control method in automatic control field. It mainly used for precise control to maintain a desired output. The principle is to combine the weighted outputs of proportional, integral, and derivative calculations within the controller to make the system output smaller and closer to the set-point value. The PID controller is used to convert the error of Δx and Δy to the weighted outputs of $p(t)$.

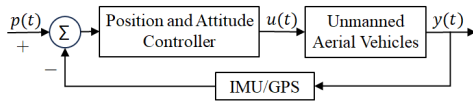


Fig. 6. The diagram of the flight control system for the UAFV.

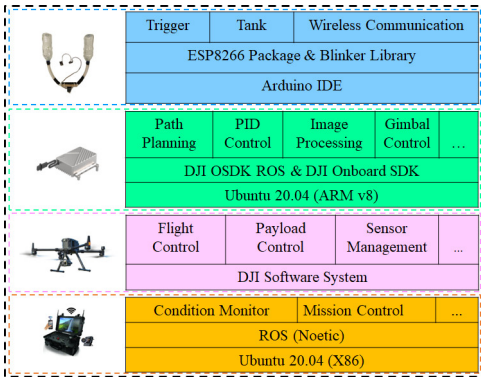


Fig. 7. The diagram of the aerial firefighting system.

D. Flight Control System

The flight control system has to control the aircraft's attitude, speed and position to ensure safety and accuracy during flight. Fig. 6 shows the diagram of a flight control system for a UAFV. It consists of sensors, actuators and controllers. Sensors are used to collect data from the real attitude and position of the UAFV. The position and attitude controllers are used to interpret the difference between the desired value $p(t)$ and the actual value and send commands to the actuators. Actuators are used to change the speed of motors to control the UAFV's attitude and position. Since the flight control system design is a mature technology and such a baseline control has been designed and embedded by DJI in the M300 UAV platform without access by users, it will not be explained in detail here.

III. SYSTEM DESIGN AND AERIAL FIREFIGHTING TESTING

In order to implement the proposed algorithm, an aerial firefighting system is designed and tested. Then the results of aerial firefighting testing is analyzed in this section.

A. The Aerial Firefighting System

Fig. 7 shows the lists of system design and corresponding functions. It includes four parts which are the water-dropping module, the UAFV and sensors module, the onboard mission computer module and the ground station module. The left column is the hardware selection for every module and the right column is the corresponding software development structures and functions.

1) *Water-dropping Module*: Water-dropping module includes a trigger and a custom tank with mechanical connectors in Fig. 8. The trigger refers to a kind of mechanism that can receive water-dropping commands from the smartphone in the ground station and convert the valve-opening command into a signal that drives servo action to the valve of

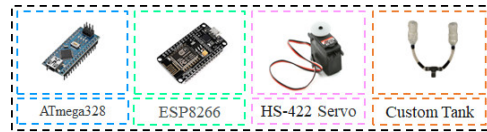


Fig. 8. The diagram of the water-dropping module.



Fig. 9. The DJI Matrice 300 RTK platform mounted with Zenmuse H20T.

the tank filled with water. It consists of a Wi-Fi microchip ESP8266 [26], a microcontroller ATmega328 [27] and a servo HS-422 [28]. The custom tank consists of two storage bottles, two pipes as Y shape and a valve connected with the servo for releasing water/retardant in the tank when needed automatically.

2) *UAFV and Sensors Module*: The UAFV plays the role that carrying various payloads and powering mechanisms and devices. Stability and reliability are very important. The DJI Matrice 300 RTK (M300) [22] is a powerful industrial and commercial UAV platform offering unparalleled flight performance and safety features [23]. So, the M300 is selected as the UAFV for our wildfire fighting mission. At the same time, the DJI Zenmuse H20T (H20T) [24], [25] is a hybrid sensor solution with 640*512 resolution and 30Hz thermal imaging camera, wide camera, zoom camera, and controllable range gimbal. H20T is engineered exclusively for the M300 platform, and it is the ultimate match for the M300. So, the infrared thermal imaging sensor of the H20T is utilized to perceive the fire spot. Fig. 9 shows a M300 platform mounted with the H20T palyload/sensor.

3) *Onboard Mission Computer Module*: In order to develop users' applications, independent mission computer aside from DJI's onboard embedded computer needs to be used. The iCrest 2.0 is used for such a purpose and it is a second-generation microcomputer with capability for DJI SDK developers to make communications with DJI embedded onboard computer for various mission applications which can help UAFV to be smarter and intelligent in multiple application scenarios. It is compatible with many DJI UAV platforms, including DJI M300 platform. The iCrest 2.0 (5G) version is equipped with NVIDIA Jetson NX module, which has rapid complex graphics processing capability, is chosen as the onboard mission computer in this work. Fig. 10 shows the connection relationship with the M300 platform and other payloads.

4) *Ground Station Module*: The ground station is made of three parts, the DJI Remote Pilot, Smartphone and Ground Station Computer. The DJI Remote Pilot can monitor various states of the M300 during missions and send controlling orders using OcuSync 2.0 digital image transmission which can cover a distance of 15 kilometers. The Smartphone can connect to the water-dropping module and send dropping



Fig. 10. The connection for the iCrest 2.0 development.



Fig. 11. The aerial firefighting systematic architecture.



Fig. 12. The equipment assembly and wildfire simulation before testing.

water orders to trigger the dropping action. The Ground Station Computer can be connected to iCrest 2.0 through a wireless router and typically sends user control instructions to initialize and start custom applications in iCrest 2.0 on the local area network.

Fig. 11 shows the whole system architecture. With the above mission-updated M300 platform, the wildfire fighting UAV is not only supplied with iCrest 2.0 for real-time calculations for the mission operation needed perception and motion planning and control, but also the trigger device to be communicated with the iCrest 2.0 for the water-dropping operation towards precise water dropping when needed to extinguish the wildfire. If an emergency occurs, the user can take over the control authority of the iCrest 2.0 using the Remoter Pilot. The ground computer is used to start and initialize the user application and is utilized to receive the task process state and water-dropping requirements. On receiving the requirement of water-dropping, the operator will send trigger commands to trigger water dropping. All the modules work together during the tasks and play different roles in each phase of wildfire fighting operation.

B. Aerial Firefighting Tests and Result Analysis

In order to verify the effectiveness of the above-mentioned system, outdoor aerial firefighting tests were conducted in the field. As can be seen, Fig. 12 shows the ultimate flight equipment assembly and wildfire simulation scenarios. The iCrest 2.0 is fixed on the top of M300 and tanks are fixed on both sides of M300. The two tanks converge to an outlet that looks to the ground vertically through the Y-pipe. Wildfire is mimicked by lighting up some woods in a container with a radius of 15 centimeters.

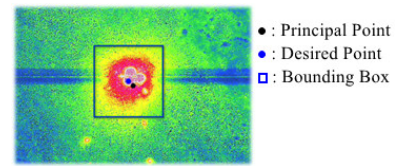


Fig. 13. An infrared thermal image at a certain moment.

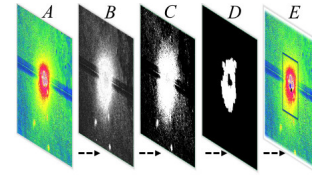


Fig. 14. The process of detecting and estimating the desired point.

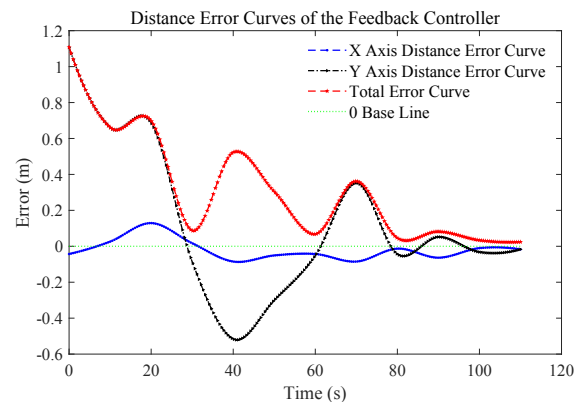


Fig. 15. The distance error curves of the feedback controller.

Fig. 13 shows an IR image at certain moment during the phase of perception and estimation of center of the fire spot. The black point is the principal point and the blue point is the estimated center of the fire spot area. It is called the desired point in the feedback controller. The blue box is the adaptive bounding box which can catch the fire spot area. The IR camera will detect the fire spot and estimate the center of the fire spot. The feedback controller will drive the M300 to approach the desired point according to the error between the desired point and the principal point. To estimate the blue point, the IR image goes through different stages of processing. Fig. 14 shows the effect of the detailed processing flow at each step. Image A is a real-time original IR image. Then it is converted to the grayscale image of B. After that, the Otsu's method is used to detect the fire spot in image B and it gets the image C. In order to estimate the center of the position of the fire spot area, erosion and dilation are used to delete noise and obtain the image D. Finally, the center position of an adaptive bounding box which can catch the detected fire spot is regarded as the estimated center of the fire spot in the image E.

Fig. 15 shows the distance error curves of the feedback controller in the camera coordinate. The depth/height z_c is set to 10 meters based on the testing and evaluation about distance between infrared camera lens and fire spot. Suppose

the X axis distance error is x_e which stands for the error between the desired point and the principal point in the camera coordinate and the Y axis distance error is y_e which has the same corresponding definition. The definition of total error T_e is (7) on the horizontal plane:

$$T_e = \sqrt{x_e^2 + y_e^2} \quad (7)$$

It can be found that the distance error along the X and Y axes decreases and the overall trend of distance error decreases gradually over time. Finally, the total error is less than 5 centimeters at 100s from the original total error more than 1 meter based on GPS navigation (test videos: <https://www.youtube.com/user/NAVConcordia>; <https://www.youtube.com/watch?v=Vc6mD42I9jY>).

IV. CONCLUSIONS

The proposed high precision and autonomous water-dropping method has improved the water-dropping precision and guaranteed the safety of aerial firefighters in wildfire aerial firefighting using unmanned aerial firefighting vehicle (UAFV). The designed UAFV system can organically and logically combine the UAFV platform, the sensor module, the water-dropping module, the ground station module and the onboard computer module, for achieving autonomy and efficiency in an aerial firefighting mission. However, the performance of high-precision water-dropping is affected by environmental interference such as wind and smoke. Moreover, the capacity of the payloads on small UAFV is limited and the high-payload platform is waited to be built for practical aerial firefighting missions. This current system is based on a quadrotor UAFV, further development and testing on a fixed-wing UAFV will be also one of our future works.

ACKNOWLEDGMENT

This work is supported in part by the CRIAQ AVITAGS project and the Natural Sciences and Engineering Research Council of Canada. Authors would like to express appreciation to the DJI developer community for their assistance in software environment setup. The authors would like to thank also to other group members for working on the AVITAGS project, including Qiaomen Qin, Erfan Dilfanian, Amin Taherzadeh, Huajun Dong, and Dr. Jie Wang for their support and help in the outdoor experiments.

REFERENCES

- [1] C. R. Proctor, J. Lee, D. Yu, A. D. Shah, and A. J. Whelton, "Wildfire caused widespread drinking water distribution network contamination," *AWWA Water Science*, vol. 2, no. 4, p. e1183, 2020.
- [2] J. C. Liu, A. Wilson, L. J. Mickley, F. Dominici, K. Ebisu, Y. Wang, M. P. Sulprizio, R. D. Peng, X. Yue, J.-Y. Son *et al.*, "Wildfire-specific fine particulate matter and risk of hospital admissions in urban and rural counties," *Epidemiology*, vol. 28, no. 1, p. 77, 2017.
- [3] D. A. DellaSala and C. T. Hanson, *The ecological importance of mixed-severity fires: Nature's Phoenix*. Elsevier, 2015.
- [4] R. J. Mangan, *Wildland firefighter fatalities in the United States: 1990-2006*. US Forest Service, Missoula Technology and Development Center, 2007.
- [5] A. A. Alkhatib, "A review on forest fire detection techniques," *International Journal of Distributed Sensor Networks*, vol. 10, no. 3, p. 597368, 2014.
- [6] U. Dampage, L. Bandaranayake, R. Wanasinghe, K. Kottahachchi, and B. Jayasanka, "Forest fire detection system using wireless sensor networks and machine learning," *Scientific Reports*, vol. 12, no. 1, p. 46, 2022.
- [7] F. A. Hossain, Y. M. Zhang, and M. A. Tonima, "Forest fire flame and smoke detection from UAV-captured images using fire-specific color features and multi-color space local binary pattern," *Journal of Unmanned Vehicle Systems*, vol. 8, no. 4, pp. 285–309, 2020.
- [8] X. Wang, H. Liu, Y. Tian, Z. Chen, and Z. Cai, "A fast optimization method of water-dropping scheme for fixed-wing firefighting aircraft," *IEEE Access*, vol. 9, pp. 120 815–120 832, 2021.
- [9] B. Aydin, E. Selvi, J. Tao, and M. J. Starek, "Use of fire-extinguishing balls for a conceptual system of drone-assisted wildfire fighting," *Drones*, vol. 3, no. 1, p. 17, 2019.
- [10] C. Yuan, Y. M. Zhang, and Z. Liu, "A survey on technologies for automatic forest fire monitoring, detection, and fighting using unmanned aerial vehicles and remote sensing techniques," *Canadian Journal of Forest Research*, vol. 45, no. 7, pp. 783–792, 2015.
- [11] F. Amon, N. Bryner, and A. Hamins, "Evaluation of thermal imaging cameras used in fire fighting applications," in *Infrared Imaging Systems: Design, Analysis, Modeling, and Testing XV*, vol. 5407, SPIE, 2004, pp. 44–53.
- [12] S. Johnson, "On digital photography," *O'Reilly*, 2006.
- [13] M. Sezgin and B. Sankur, "Survey over image thresholding techniques and quantitative performance evaluation," *Journal of Electronic Imaging*, vol. 13, no. 1, pp. 146–168, 2004.
- [14] K. R. Castleman, *Digital image processing*. Prentice Hall Press, 1996.
- [15] S. Suzuki *et al.*, "Topological structural analysis of digitized binary images by border following," *Computer Vision, Graphics, and Image Processing*, vol. 30, no. 1, pp. 32–46, 1985.
- [16] Y. Zheng, J. Li, and L. Wu, "Tree radial growth measurement system based on line structured light vision," in *IEEE International Conference on Power, Intelligent Computing and Systems (ICPICS)*, 2019, pp. 338–342.
- [17] Z. Zhang, "Flexible camera calibration by viewing a plane from unknown orientations," in *Proceedings of the Seventh IEEE International Conference on Computer Vision*, 1999, pp. 666–673.
- [18] Z. Zhang, "A flexible new technique for camera calibration," *IEEE Transactions on Pattern Analysis and Machine Intelligence*, vol. 22, no. 11, pp. 1330–1334, 2000.
- [19] I. N. Swamidoss, A. B. Amro, and S. Sayadi, "Systematic approach for thermal imaging camera calibration for machine vision applications," *Optik*, vol. 247, p. 168039, 2021.
- [20] R. Szeliski, *Computer vision: Algorithms and applications*. Springer Nature, 2022.
- [21] R. Hartley and A. Zisserman, *Multiple view geometry in computer vision*. Cambridge University Press, 2003.
- [22] S. Czyża, K. Szuniewicz, K. Kowalczyk, A. Dumalski, M. Ogrodniczak, and Ł. Zieleniewicz, "Assessment of accuracy in unmanned aerial vehicle (UAV) pose estimation with the real-time kinematic (RTK) method on the example of DJI Matrice 300 RTK," *Sensors*, vol. 23, no. 4, p. 2092, 2023.
- [23] T. Kersten, J. Wolf, and M. Lindstaedt, "Investigations into the accuracy of the UAV system DJI Matrice 300 RTK with the sensors zenmuse P1 and L1 in the hamburg test field," in *XXIV ISPRS Congress Imaging Today, Foreseeing Tomorrow*, June 6–11, 2022, Nice, France, 2022, pp. 339–346.
- [24] S. Li, L. Qiao, Y. M. Zhang, and J. Yan, "An early forest fire detection system based on DJI M300 drone and H20T camera," in *2022 International Conference on Unmanned Aircraft Systems (ICUAS)*, June 21–24, 2022, Dubrovnik, Croatia, pp. 932–937.
- [25] E. I. Parisi, A. Masiero, G. Tucci, I. Cortesi, and F. Mugnai, "Thermal camera geometric self-calibration supported by RTK measurements," in *2022 IEEE Workshop on Metrology for Agriculture and Forestry (MetroAgriFor)*, 2022, pp. 249–254.
- [26] J. Mesquita, D. Guimarães, C. Pereira, F. Santos, and L. Almeida, "Assessing the esp8266 wifi module for the internet of things," in *IEEE 23rd International Conference on Emerging Technologies and Factory Automation (ETFA)*, 2018, pp. 784–791.
- [27] M. Umer and M. M. Khan, "Smart home automation using atmega328," *Advanced Journal of Science and Engineering*, vol. 1, no. 3, pp. 86–90, 2020.
- [28] A. U. Haque, H. Kabir, S. C. Banik, and M. T. Islam, "Development of a voice controlled robotic arm," 2023, arXiv:2303.09645.